

Manifestation of quantum-billiard eigenvalue statistics from subthreshold emission of vertical-cavity surface-emitting lasers

Y. F. Chen,* Y. T. Yu, P. Y. Chiang, P. H. Tuan, Y. J. Huang, H. C. Liang, and K. F. Huang
Department of Electrophysics, National Chiao Tung University, 1001 Ta-Hsueh Road, Hsinchu 30050, Taiwan
 (Received 4 October 2010; published 11 January 2011)

We report that the subthreshold emission spectra of vertical-cavity surface-emitting lasers (VCSELs) can be analogously used to manifest the quantum-billiard energy spectra. The Fourier-transformed distributions of the subthreshold emission spectra are demonstrated to display various peak structures that are in good agreement with the results of the quantum-billiard model. We also verify that the statistical analyses of the nearest-neighbor eigenvalue spacing distributions obey a Poisson distribution for an equilateral-triangular device and a Wigner distribution for a stadium-shaped device.

DOI: [10.1103/PhysRevE.83.016208](https://doi.org/10.1103/PhysRevE.83.016208)

PACS number(s): 05.45.Mt, 42.65.Sf, 42.55.Sa

I. INTRODUCTION

Quantum manifestations of classical chaos recurrently attract much attention because the experimental techniques exploring the quantum classical correspondence have been continuously improved [1–4]. The two-dimensional (2D) billiard problem is particularly useful for studying the classical behaviors in the corresponding quantum regime due to their simplicity [5,6]. Ballistic-electron transport in quantum dots is often regarded as experimental realizations of quantum billiards [7–9]. The similarity between Schrödinger and Helmholtz equations has been widely used to develop electromagnetic wave resonators, ranging from 2D microwave cavities [10–12] to optical microdisk lasers [13–15], as another class of experimental and theoretical quantum-chaotic model systems.

Recently, the lateral oxide confinements of the vertical-cavity surface-emitting lasers (VCSELs) with a unique longitudinal wave vector k_z have been justified to be equivalent to 2D wave billiards with hard walls [16]. The special superiority of oxide-confined VCSELs is that the unique longitudinal wave vector k_z brings out the lasing transverse modes to be directly reimaged with simple optics for analogous observations of 2D quantum-billiard wave functions. More recently, Gensty *et al.* [17] utilized the emission spectra far above lasing threshold to analyze the eigenvalue spacing distribution and confirmed the oxide-confined VCSELs to be fascinating devices for wave chaos studies. However, the mode-competition phenomena usually induce mode-hopping instability and only several tens of cavity modes can be simultaneously lasing in the emission spectra far above lasing threshold. So far, the VCSEL devices have never been successfully employed to manifest the signatures of classical chaos and the role of periodic orbits in the quantum-billiard spectra.

Shortly after the invention of the semiconductor laser early in the 1960s, it was found that several hundreds to a thousand cavity modes could be clearly observed just below the lasing threshold in conventional edge-emitting semiconductor lasers [18,19]. In the same way, it was recently demonstrated that the oxide-confined VCSELs could emit several hundreds of

transverse modes in the subthreshold emission spectra [20]. This result casts light on the prospect of using the VCSEL device to realize the experimental manifestations of classical chaos in the quantum-billiard spectra.

In this work we first employ a large-aperture equilateral-triangular VCSEL to explore the subthreshold emission spectrum and the Fourier transformed length spectrum. It is found that the experimental length spectrum agrees very well with the result of the quantum-billiard model to exhibit a series of sharp peaks at multiples of the lengths of the primitive periodic orbits. Furthermore, we use the subthreshold emission spectrum in a stadium-shaped VCSEL to investigate the signatures of wave chaos. Experimental results noticeably reveal that the isolated periodic orbits, corresponding to the so-called scar modes, play an essential role in the genuine chaotic wave resonators. We also confirm that the nearest-neighbor eigenvalue spacing distributions for the equilateral-triangular and stadium-shaped VCSELs obey a Poisson distribution and a Wigner distribution, respectively.

II. PERIODIC-ORBIT THEORY

Periodic-orbit theory developed by Gutzwiller [5] and Balian and Bloch [21] has been extensively used to analyze the long-range correlations in quantum spectra [22–24]. Here we give a brief synopsis for the application of periodic-orbit theory on the analysis of quantum-billiard spectra. Mathematically, the energy level density $\rho_o(E)$ can be split into a smoothly varying part $\rho(E)$ and a remaining oscillatory part. According to the Gutzwiller trace formula, the oscillatory part of the eigenvalue density is given by the actions of classical orbits, $S_\mu(E)$. Therefore the energy level density $\rho(E)$ can be expressed as

$$\begin{aligned} \rho(E) &= \sum_{n=1}^{\infty} \delta(E - E_n) \\ &= \rho_o(E) + \sum_{v=1}^{\infty} \sum_{\mu} \rho_{v,\mu} \cos \left[v \left(\frac{S_\mu(E)}{\hbar} - \phi_\mu \right) \right], \quad (1) \end{aligned}$$

where the index μ labels the periodic orbits and $v = 1, 2, \dots$ run over all recurrences of such orbits. For quantum-billiard systems, the action $S_\mu(E)/\hbar$ is given through the term kL_μ , where k is the wave number and L_μ is the path length of the periodic orbit. The eigenvalue density for the billiard

*Author to whom correspondence should be addressed.
 yfchen@cc.nctu.edu.tw

problem can be expressed as $\sum_{n=1}^{\infty} \delta(k - k_n)$, where k_n are the quantized wave numbers. As a result, the Fourier-transformed spectrum of the eigenvalue density is given by

$$\begin{aligned} \rho_{\text{FT}}(L) &= \sum_{n=1}^{\infty} \int_{-\infty}^{\infty} \delta(k - k_n) e^{ikL} = \sum_{n=1}^{\infty} e^{ik_n L} \\ &= \sum_{\nu=1}^{\infty} \sum_{\mu} \rho_{\nu,\mu} \delta(L - \nu L_{\mu}). \end{aligned} \quad (2)$$

Equation (2) indicates that the length spectrum $\rho_{\text{FT}}(L)$ will display a series of intense peaks at multiples of the lengths of the periodic orbits, i.e., at $L = \nu L_{\mu}$. In other words, the character of classical periodic orbits can be revealed in the Fourier-transformed spectrum of the eigenvalue density. For numerical evaluation, the length spectrum can be written as $\rho_N(L) = \sum_{n=1}^N e^{ik_n L}$, where N should be large but finite.

III. EXPERIMENTAL RESULTS AND THEORETICAL ANALYSIS

The experimental VCSEL devices were grown with metal-organic chemical vapor deposition. Each device consists of a multiple quantum-well active region and a vertical cavity formed by two distributed Bragg reflector (DBR) mirrors. The active region comprises three $\text{Al}_{0.07}\text{Ga}_{0.93}\text{As}-\text{Al}_{0.36}\text{Ga}_{0.64}\text{As}$ quantum wells with well and barrier thickness of 70 and 100 Å, respectively. The spacers at both sides of quantum well were added to form a $1-\lambda$ cavity. The longitudinal wave number is given by $k_z = 2\pi/\lambda_o$ and the values of λ_o are designed to be approximately 782.6 nm for the experimental devices. The periods for the top and bottom DBR mirrors are 23 and 29, respectively. A high-Al composition $\text{Al}_{0.97}\text{Ga}_{0.03}\text{As}$ layer was placed at the first p -type doped DBR mirror and was oxidized to define an aperture for current confinement. This oxide aperture simultaneously induces an optical confinement because of the large difference of the refractive index between the semiconductor material and the oxide layer, thus forming an essentially rigid wall waveguide [16,17]. Here we fabricated two different shapes of oxide apertures, an equilateral-triangular shape and a stadium shape, to explore the signature of wave chaos in the subthreshold emission spectra. The optical microscope photographs of the experimental VCSELs are shown in Fig. 1.

The VCSEL device was placed in a temperature-controlled system with a stability of 0.1 °C near room temperature. We employed an optical spectrum analyzer based on a Michelson interferometer to measure the subthreshold emission spectra with a resolution up to 0.002 nm. With the relation of $k_z = 2\pi/\lambda_o$, the subthreshold emission spectrum $\rho(\lambda)$ can be changed from a function of the emission wavelength λ to a function of the transverse wave number k by using the relation $k = \sqrt{(2\pi/\lambda)^2 - k_z^2}$. We first investigate the subthreshold emission spectrum of an equilateral-triangular VCSEL with the side length of $a = 66 \mu\text{m}$, as shown in Fig. 1(a). Figure 2(a) shows the experimental emission spectrum $\rho(k)$ of the equilateral-triangular VCSEL just below the lasing threshold. With the experimental data, the Fourier transform of the subthreshold spectrum $\rho_{\text{FT}}(L)$ can be numerically calculated.

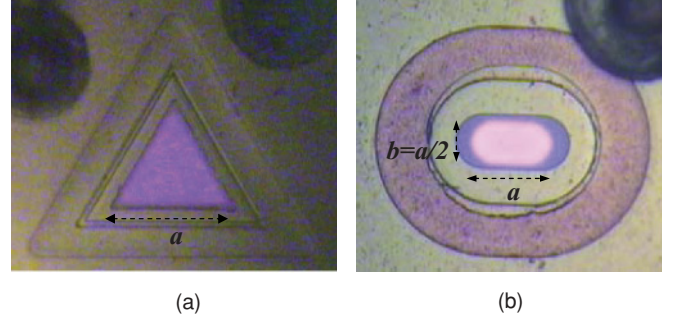


FIG. 1. (Color online) Optical microscope photographs of the experimental VCSELs for (a) equilateral-triangular device with $a = 66 \mu\text{m}$ and (b) stadium-shaped device with $a = 42 \mu\text{m}$ and $b = 21 \mu\text{m}$.

Figure 2(b) depicts the calculated results for the path-length spectrum $|\rho_{\text{FT}}(L)|^2$ corresponding to the experimental data shown in Fig. 2(a). We experimentally found that there was no obvious difference in the path-length spectra from sample to sample for device growth in the same batch. To make a comparison with the quantum-billiard spectrum, we calculated the Fourier transform of the density of states for an equilateral-triangular quantum billiard. The quantized wave numbers in an equilateral-triangular quantum billiard of side a can be analytically given by [25,26] $k_{m,n} = (4\pi/3a)\sqrt{m^2 + n^2 - mn}$ for integral values of m and n , with the restriction that $m \geq 2n$. The length spectrum was numerically calculated with the expression $\rho_N(L) = \sum_{n=1}^N \sum_{m=2n}^{2N} e^{ik_{m,n}L}$ and $N = 15$. Figure 2(b) depicts the calculated results for the billiard model.

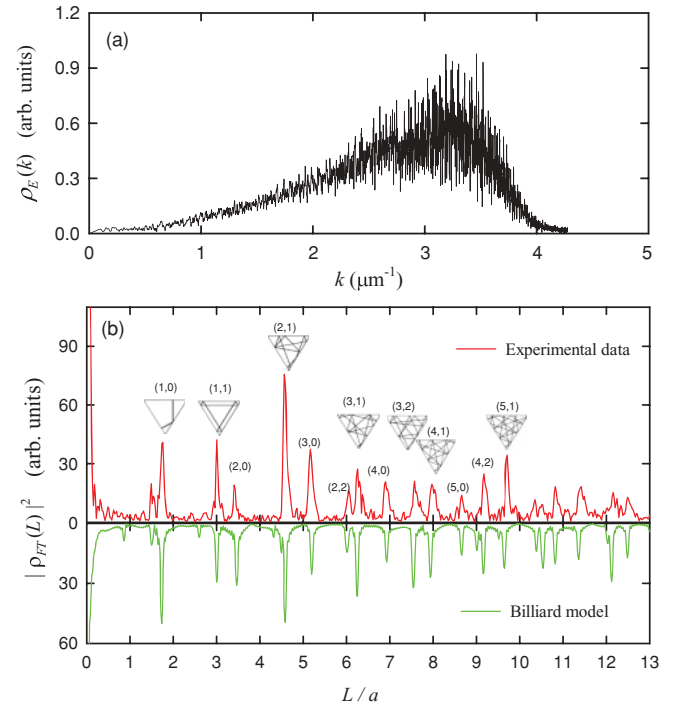


FIG. 2. (Color online) (a) Experimental emission spectrum $\rho(k)$ of the equilateral-triangular VCSEL just below the lasing threshold; (b) Fourier-transformed spectrum $|\rho_{\text{FT}}(L)|^2$. The experimental and numerical results are displayed as mirror images.

Note that the path length of the periodic orbit (p, q) can be expressed as $L_{PO}(p, q) = a\sqrt{3}\sqrt{p^2 + pq + q^2}$. If p and q have common factors, such an orbit categorically corresponds to a recurrence of a simpler one in which the particle undergoes two or more periods. It can be seen that the experimental length spectrum agrees very well with the theoretical spectrum of the billiard model to exhibit a series of sharp peaks at multiples of the lengths of the primitive periodic orbits. This good agreement signifies the feasibility of exploiting the spontaneous emission spectra of large-aperture VCSELs to investigate the energy spectra of quantum billiards in an analogous way. In earlier times, the energy spectra of quantum billiards have been successfully studied by flat microwave resonators [4,10–12]. Here we manifest the quantum-billiard path-length spectra from the active devices in the optical regime. The observation of numerous cavity modes with narrow linewidth implies that the subthreshold emission spectra of VCSELs may be useful in developing wide-band tunable light sources for optical data communication.

Next, we fabricated a VCSEL, which has the shape of a Bunimovich stadium billiard, as shown in Fig. 1(b), with the dimensions $a = 42 \mu\text{m}$ and $b = 21 \mu\text{m}$, corresponding to $\gamma = (a - b)/b = 1$. Figure 3(a) shows the experimental emission spectrum $\rho(k)$ of the stadium-shaped VCSEL just below the lasing threshold. Figure 3(b) depicts the calculated result for the Fourier-transformed spectrum $|\rho_{FT}(L)|^2$ of the experimental data shown in Fig. 3(a). To make a comparison with the quantum-billiard spectrum, we employed the so-called expansion method [27] to calculate the theoretical eigenvalue density for the stadium billiard with the same geometry. The numerical result of the quantum-billiard model

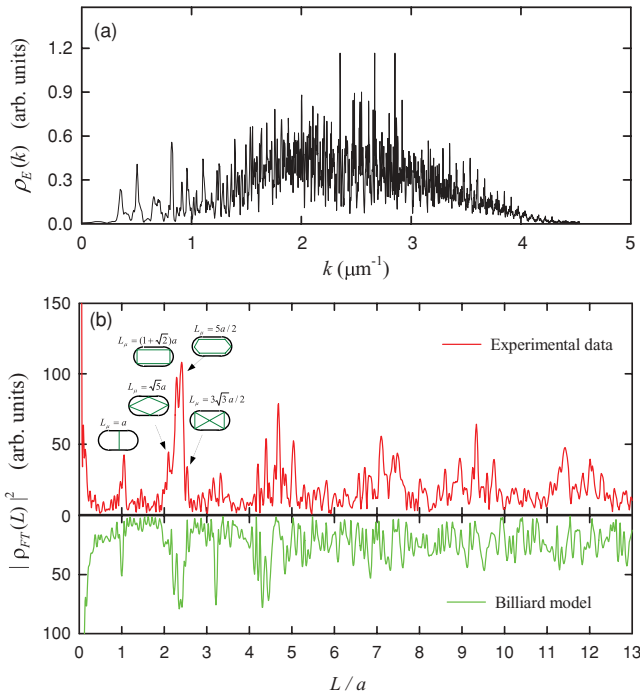


FIG. 3. (Color online) (a) Experimental emission spectrum $\rho(k)$ of the stadium-shaped VCSEL just below the lasing threshold; (b) Fourier-transformed spectrum $|\rho_{FT}(L)|^2$. The experimental and numerical results are displayed as mirror images.

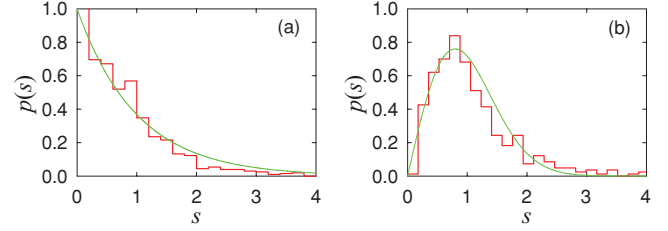


FIG. 4. (Color online) Experimental statistics for the nearest-neighbor eigenvalue spacing distribution $p(s)$ in form of histogram for (a) equilateral-triangular device and (b) stadium-shaped device. The curves represent (a) a Poisson distribution and (b) a Wigner distribution.

is shown in Fig. 3(b). It can be seen that the positions of the experimental peaks for the short-range periodic orbits, $(L/a) < 3.0$, agree well with the theoretical analysis. The short-range periodic orbits are associated with the scar modes that are numerically found to be rather insensitive to the geometry imperfection. For the long-range length distribution, the experimental spectrum comes close to the theoretical one to exhibit the complicated oscillations without conspicuous peaks. Numerical results indicate that the detailed structure in the long-range length distribution is more or less changed by the tiny perturbation, even though the salient feature of the complicated oscillations is quite similar. Therefore it is somewhat problematic to make a more quantitative comparison between the experimental and theoretical peaks for the long-range periodic orbits. Nevertheless, it is judiciously confirmed that the subthreshold emission spectra of the VCSELs with classically chaotic shape can manifest the path-length distributions to be in good agreement with the characteristics of the quantum-billiard model.

Finally, we employed the experimental emission spectra of the VCSELs to perform a statistical analysis. We searched all the peak positions in the experimental spectra and recorded these wave numbers as the sequence of eigenvalues $\{k_1, k_2, \dots, k_i, \dots\}$. The spacings $s_i = (k_{i+1} - k_i)/\Delta k$ between adjacent eigenvalues were subsequently obtained by calculating the mean spacing Δk . We obtained 817 and 548 spacings of eigenmodes for the equilateral-triangular and stadium-shaped VCSELs, respectively. Figure 4 shows the experimental statistics for the nearest-neighbor eigenvalue spacing distribution $p(s)$ in the form of a histogram. It can be seen that the statistical results for the equilateral-triangular and stadium-shaped VCSELs are in good agreement with a Poisson distribution $p(s) = \exp(-s)$ and a Wigner distribution $p(s) = (\pi s/2) \exp(-\pi s^2/4)$, respectively. The good consistency of the experimental statistics with the theoretical prediction further confirms that the subthreshold emission spectra of VCSELs can be analogously used to manifest the quantum-billiard spectra.

IV. CONCLUSIONS

In conclusion, we have investigated the manifestation of quantum-billiard energy spectra from the subthreshold emission spectra of equilateral-triangular and stadium-shaped VCSELs. The Fourier-transformed path length distribution for an equilateral-triangular VCSEL exhibits various peak

structures to be in good agreement with the results of the quantum-billiard model. We also employed a stadium-shaped VCSEL to manifest the path-length distribution corresponding to the characteristics of the quantum chaotic billiards. Furthermore, the statistical analyses of the nearest-neighbor eigenvalue spacing distributions have been verified to obey a Poisson distribution for the equilateral-triangular device and a Wigner distribution for the stadium-shaped device.

The good agreement confirms that the subthreshold emission spectra of VCSELs can be analogously used to manifest the quantum-billiard spectra.

ACKNOWLEDGMENT

This work was supported by the National Science Council of Taiwan (Contract No. NSC-97-2112-M-009-016-MY3).

-
- [1] H. J. Stöckmann, *Quantum Chaos—An Introduction* (University Press, Cambridge, England, 1999).
 - [2] T. Guhr, A. Müller-Groeling, and H. A. Weidenmüller, *Phys. Rep.* **299**, 189 (1998).
 - [3] *Quantum Chaos Y2K—The 116th Nobel Symposium*, edited by K.-F. Berggren, P. Omling, and S. Åberg [*Physica Scripta*, **T90**, 11 (2001)].
 - [4] U. Kuhl, *Eur. Phys. J. Special Topics* **145**, 103 (2007).
 - [5] M. C. Gutzwiller, *Chaos in Classical and Quantum Mechanics* (Springer-Verlag, New York, 1990).
 - [6] O. Bengtsson, J. Larsson, and K. F. Berggren, *Phys. Rev. E* **71**, 056206 (2005).
 - [7] C. M. Marcus, A. J. Rimberg, R. M. Westervelt, P. F. Hopkins, and A. C. Gossard, *Phys. Rev. Lett.* **69**, 506 (1992).
 - [8] K. F. Berggren and Z. L. Ji, *Chaos* **6**, 543 (1996).
 - [9] C. W. J. Beenakker, *Rev. Mod. Phys.* **69**, 731 (1997).
 - [10] H. J. Stöckmann and J. Stein, *Phys. Rev. Lett.* **64**, 2215 (1990).
 - [11] S. Sridhar, *Phys. Rev. Lett.* **67**, 785 (1991).
 - [12] A. Richter, *Found. Phys.* **31**, 327 (2001).
 - [13] J. U. Nöckel and D. Stone, *Nature (London)* **385**, 45 (1997).
 - [14] C. Gmachl, F. Capasso, E. E. Narimanov, J. U. Nöckel, A. D. Stone, J. Faist, D. L. Sivco, and A. Y. Cho, *Science* **280**, 1556 (1998).
 - [15] T. Harayama, P. Davis, and K. S. Ikeda, *Phys. Rev. Lett.* **90**, 063901 (2003).
 - [16] K. F. Huang, Y. F. Chen, H. C. Lai, and Y. P. Lan, *Phys. Rev. Lett.* **89**, 224102 (2002).
 - [17] T. Gensty, K. Becker, I. Fischer, W. Elsässer, C. Degen, P. Debernardi, and G. P. Bava, *Phys. Rev. Lett.* **94**, 233901 (2005).
 - [18] M. I. Nathan, A. B. Flower, and G. Burns, *Phys. Rev. Lett.* **11**, 152 (1963).
 - [19] H. S. Sommers, *J. Appl. Phys.* **44**, 1263 (1973).
 - [20] Y. F. Chen, Y. T. Yu, Y. J. Huang, P. Y. Chiang, K. W. Su, and K. F. Huang, *Opt. Lett.* **35**, 2723 (2010).
 - [21] R. Balian and C. Bloch, *Ann. Phys. (NY)* **60**, 401 (1970); **64**, 271 (1971); **69**, 76 (1970); **85**, 514 (1974).
 - [22] D. Wintgen, *Phys. Rev. Lett.* **58**, 1589 (1987).
 - [23] I. V. Zozoulenko, A. S. Sachrajda, P. Zawadzki, K. F. Berggren, Y. Feng, and Z. Wasilewski, *Semicond. Sci. Technol.* **13**, A7 (1998).
 - [24] L. Christensson, H. Linke, P. Omling, P. E. Lindelof, I. V. Zozoulenko, and K. F. Berggren, *Phys. Rev. B* **57**, 12306 (1998).
 - [25] M. V. Berry and M. Wilkinson, *Proc. R. Soc. London, Ser. A* **392**, 15 (1984).
 - [26] M. Brack and R. K. Bhaduri, *Semiclassical Physics* (Addison-Wesley, Reading, MA, 1997).
 - [27] D. L. Kaufman, I. Kosztin, and K. Schulten, *Am. J. Phys.* **67**, 133 (1999).